Self-Referencing Spectral Interferometry for Measuring Ultrashort Optical Pulses

Chris Iaconis and Ian A. Walmsley

(Invited Paper)

***Abstract*—This paper describes a novel self-referencing interferometric method for measuring the time-dependent intensity and phase of ultrashort optical pulses. The technique, spectral phase interferometry for direct electric-field reconstruction (SPIDER), measures the interference between a pair of spectrally sheared replicas of the input pulse. Direct (noniterative) inversion of the interferogram yields the electric field of the input pulse without ambiguity. The interferogram, which is solely a function of frequency, is resolved with a spectrometer and recorded with a slow detector. Moreover, the geometry is entirely collinear and requires no moving components. This paper describes in detail the principle of operation, apparatus, and calibration of SPIDER and gives experimental examples of reconstructed pulses.**

***Index Terms*— Pulse characterization, pulse measurements, pulse reconstruction, ultrafast optics.**

I. Introduction

THERE ARE three known strategies for measuring the electric field of optical pulses; spectrography, tomography, and interferometry [1], [2]. The most common of these, spectrographic techniques, such as frequency-resolved optical gating (FROG) [3], temporal analysis of spectral components (TASC) [4], frequency-domain phase measurements (FDPM) [5], and spectrally and temporally resolved upconversion technique (STRUT) [6], measure a two-dimensional (2-D) representation of the one-dimensional (1-D) field and consequently require the collection of a relatively large amount of data. Moreover, unless the pulse has a simple structure, spectrography requires sophisticated iterative data inversion algorithms to reconstruct the field. Tomography also requires a large 2-D data set, but data inversion is direct (noniterative). In practice, however, it is difficult to fabricate a tomographic apparatus with a bandwidth of several terahertz and, consequently, tomography has not been applied to ultrafast pulses, although tomographic-like methods that require iterative inversion have been demonstrated [7]. Interferometry, in contrast, requires only a 1-D data set to reconstruct a 1-D field and uses direct data inversion to do so. Diels has demonstrated an interferometric method that uses an ultrafast photodiode and Schottky diode nonlinear mixer to record the beat notes between pairs of spectral components of the input pulse [8]. Similarly, direct optical spectral phase measurement (DOSPM) [9] uses a nonlinear time gate to record the interference beats. Because data collection requires either a fast detector or a fast nonlinear time gate, neither of these techniques has seen widespread use.

This paper describes an interferometric method for characterizing ultrashort optical pulses that does not rely on a fast detector or a fast time gate and still uses direct data inversion. The technique, spectral phase interferometry for direct electric-field reconstruction (SPIDER), is a specific implementation of spectral shearing interferometry [10], [11]. SPIDER uses nonlinear frequency mixing to generate a pair of identical but frequency-sheared replicas of the input pulse. The interference between this pair of pulses is recorded easily with a spectrometer followed by an integrating (i.e., slow) detector. Moreover, the geometry is entirely collinear, the apparatus requires no moving components, and the direct inversion routine is simple, rapid, and robust. Section II of this paper describes the relationship between the electric field that describes an optical pulse and its analytic signal and defines the related quantities such as the time-dependent intensity, time-dependent phase, and absolute phase. Section III describes the principles of spectral shearing interferometry and details the data inversion routine used with SPIDER. Finally, Section IV describes the components and calibration of the SPIDER apparatus and provides examples of pulses reconstructed from experimental data.

II. Describing an Optical Pulse by its Analytic Signal

The real electric field $\varepsilon(t)$ underlying an optical pulse is twice the real part of its analytic signal $E(t)$: $\varepsilon(t) = 2 \times \mathrm{Re}[E(t)]$. The analytic signal is the single-sided inverse Fourier transform of the Fourier transform of the field

$$E(t) = \int_0^\infty d\omega\, \tilde{\varepsilon}(\omega) \exp[-i\omega t] \tag{1}$$

where

$$\tilde{\varepsilon}(\omega) = \int_{-\infty}^\infty dt\, \varepsilon(t) \exp[i\omega t]. \tag{2}$$

The electric field is considered to have compact support in the time domain and is further assumed to have no spectral component at $\omega = 0$, so $\tilde{\varepsilon}(\omega = 0) = 0$. The analytic signal

Manuscript received November 16, 1998; revised January 5, 1999.

C. Iaconis is with the Institute of Optics, University of Rochester, Rochester, NY 14627 USA. He is also with USAF Phillips Laboratory, AFRL/DELO, Kirtland AFB, NM 87117 USA.

I. A. Walmsley is with the Institute of Optics, University of Rochester, Rochester, NY 14627 USA.

Publisher Item Identifier S 0018-9197(99)02549-X.

is complex and therefore can be expressed uniquely in terms of an amplitude and phase

$$E(t) = |E(t)| \exp[i\phi_t(t)] \exp[i\phi_0] \exp[-i\omega_0 t] \tag{3}$$

where $|E(t)|$ is the time-dependent envelope, ω_0 is the carrier frequency (usually chosen near the center of the pulse spectrum), $\phi_t(t)$ is the time-dependent phase, and ϕ_0 is the absolute phase. The square of the envelope $|E(t)|^2$ is the time-dependent intensity of the pulse. The time-dependent phase accounts for the occurrence of different frequencies at different times, and the absolute phase specifies the position of the carrier relative to the envelope.

Since the pulse has no dc spectral component, the electric field must have zero area: $\int_{-\infty}^{\infty} dt\, \varepsilon(t) = 0$. As a result, the absolute phase of the pulse is fixed once the envelope, time-dependent phase, and carrier frequency are specified. In practice, though, unless the pulse duration is close to a single cycle, ϕ_0 changes dramatically in response to immeasurably small changes in the envelope. Consequently, pulse characterization devices should strive to measure the absolute phase as if it were a free parameter. We note parenthetically that none of the pulse measurement techniques demonstrated to date, including SPIDER, return the absolute phase.

The frequency representation of the analytic signal is the Fourier transform of $E(t)$

$$\tilde{E}(\omega) = \int_{-\infty}^{\infty} dt E(t) \exp[i\omega t] = \begin{Bmatrix} \tilde{\varepsilon}(\omega), & \omega > 0 \\ 0, & \omega \le 0 \end{Bmatrix}. \tag{4}$$

$\tilde{E}(\omega)$ is often expressed as

$$\tilde{E}(\omega) = |\tilde{E}(\omega)| \exp[i\phi_\omega(\omega)] \exp[i\phi_0] \tag{5}$$

where $|\tilde{E}(\omega)|$ is the spectral amplitude, $\phi_\omega(\omega)$ is the spectral phase, and ϕ_0 is the absolute phase. The square of the spectral amplitude $|\tilde{E}(\omega)|^2$ is the spectral intensity—the familiar quantity measured with a spectrometer—and the spectral phase describes the relative phases of all the frequencies.

To reconstruct the electric field, one need only measure its Fourier transform for a finite set of frequencies. The Whittaker–Shannon sampling theorem [12] asserts that, if the field has compact support in the time domain over a range $N \times \Delta t$, then a sampling of $\tilde{E}(\omega)$ at the Nyquist frequency interval of $2\pi/N\Delta t$ is sufficient for reconstructing the analytic signal $E(t)$ and, consequently, the electric field $\varepsilon(t)$ exactly.

III. SPIDER: A Spectral Shearing Interferometer

A. The Principles of Spectral Shearing

The fastest photodetectors cannot directly measure the envelope, much less the carrier, of ultrafast optical pulses. It is possible, though, to use slow photodetectors, provided a set of linear filters of known response functions are available. One simply records the output energy as a function of the filter parameters (such as the center of the passband of a spectrometer, for instance). Two classes of linear filter are both necessary and sufficient for measuring the electric field of optical pulses: time stationary filters, in which the time of incidence of the input pulse does not affect the output, and frequency stationary filters, the output of which is unchanged by arbitrary frequency shifts of the input. Filters from these two classes can be combined to synthesize a linear filter of arbitrary response. Moreover, these are the only filters that have been used to date in pulse-shape measurement and are the easiest to implement in practice.

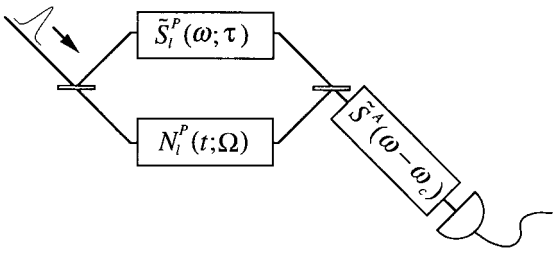

Fig. 1. A generalized spectral shearing interferometer. The input pulse is split into two replicas at a beamsplitter. One replica is delayed by a linear spectral phase modulator (upper path) and the other replica is frequency shifted by a linear temporal phase modulator (lower path). The filtered pulses are recombined on the second beamsplitter and the resulting interferogram is resolved with a spectrometer.

There are two additional important filter specializations: amplitude-only and phase-only. These filters behave as their names suggest; the former provides amplitude modulation while the later modulates only phase. An example of an amplitude-only time-stationary filter is the spectrometer, whose idealized transfer function is

$$\tilde{S}^A(\omega;\omega_c) = \exp[-(\omega-\omega_c)^2/(2\gamma^2)] \tag{6}$$

where ω_c is the center frequency and γ is the frequency passband. S denotes that this filter is time-stationary and the superscript A indicates that it is an amplitude filter. Since even modest spectrometers have resolutions significantly better than a terahertz, they can easily resolve the spectral intensity of ultrashort optical pulses. But, to measure phase, one needs at least two linear filters—one time-stationary and one frequency-stationary. Spectral shearing relies on an interferometric arrangement of such filters.

A schematic spectral shearing interferometer is shown in Fig. 1. The interferometer consists of in-parallel phase filters, one linear temporal phase modulator and one linear spectral phase modulator, followed by a spectrometer. A beamsplitter generates two replicas of the input pulse. One pulse replica passes through the temporal phase modulator and the other passes through the spectral phase modulator. The filtered pulses are recombined on a second beamsplitter and the resulting signal is resolved with a spectrometer. Since the spectrometer is a time-stationary device, the key linear phase filter is the frequency-stationary temporal phase modulator. The temporal phase modulator shifts the spectrum of the input pulse by Ω. Its response function is

$$N_l^P(t;\Omega) = \exp[-i\Omega t] \tag{7}$$

where N denotes that this filter is time nonstationary, the superscript P indicates that it is a phase filter, and the subscript l specifies that the phase modulation is linear. Likewise, the transfer function of the spectral phase modulator is

$$\tilde{S}_l^P(\omega;\tau) = \exp[i\tau\omega]. \tag{8}$$

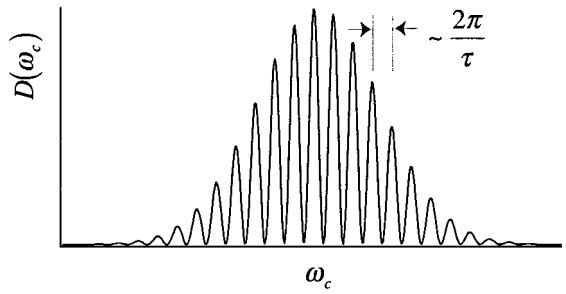

Fig. 2. Simulated spectral interferogram of the interference of a pair of spectrally sheared pulses. The pulses are delayed with respect to one another by τ and, consequently, the nominal fringe spacing is $2\pi/\tau$. Spectral phase of the input pulse manifests itself as variations from the nominal fringe spacing.

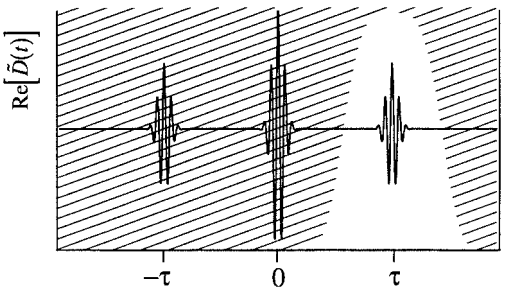

Fig. 3. The Fourier transform of the interferogram of Fig. 2. The Fourier transform is complex but only the real part is shown. The desired phase information is contained in the component centered near $+\tau$. This component is isolated by multiplying the Fourier transform (both the real and imaginary quadratures) by a filter function centered at $+\tau$.

This filter simply delays an input pulse by τ. The signal obtained after the combined pulses are passed through the spectrometer is

$$D(\omega_c;\Omega,\tau) = \int d\omega \Big| \tilde{S}^A(\omega-\omega_c) \cdot \left\{ \left[\int d\omega' \tilde{N}_l^P(\omega'-\omega)\tilde{E}(\omega') \right] + \tilde{S}_l^P(\omega)\tilde{E}(\omega) \right\} \Big|^2. \tag{9}$$

Since the spectral shift and the temporal delay are fixed, the only variable is the center frequency of the spectrometer. Furthermore, the spectrometer usually has a passband much narrower than the spectrum of the input pulse. In this case, the square of its transfer function is reliably approximated by a delta function $|\tilde{S}^A(\omega-\omega_c)|^2 \approx \delta(\omega-\omega_c)$, and the signal is simply

$$D(\omega_c) = |\tilde{E}(\omega_c-\Omega)|^2 + |\tilde{E}(\omega_c)|^2 + 2|\tilde{E}(\omega_c-\Omega)\tilde{E}(\omega_c)|\cos[\phi_\omega(\omega_c-\Omega) - \phi_\omega(\omega_c) - \tau\omega_c]. \tag{10}$$

$D(\omega_c)$ is a standard shearing interferogram consisting of fringes nominally spaced in frequency at $2\pi/\tau$. A simulated interferogram is shown in Fig. 2. The spectral phase of the input pulse, in the form of the phase difference $\phi_\omega(\omega_c-\Omega)-\phi_\omega(\omega_c)$ between two different frequency components of the test pulse, manifests itself as perturbations from the nominal fringe spacing.

B. Inverting the Data

The spectral phase is extracted from the interferogram of (10) by analyzing the relative positions of the fringes. To simplify the analysis, we write the interferogram as

$$D(\omega_c) = D^{(\mathrm{dc})}(\omega_c) + \exp[-i\tau\omega_c]D^{(-\mathrm{ac})}(\omega_c) + \exp[i\tau\omega_c]D^{(+\mathrm{ac})}(\omega_c) \tag{11}$$

where

$$D^{(\mathrm{dc})}(\omega_c) = |\tilde{E}(\omega_c-\Omega)|^2 + |\tilde{E}(\omega_c)|^2 \tag{12}$$

$$D^{(-\mathrm{ac})}(\omega_c) = |\tilde{E}(\omega_c-\Omega)\tilde{E}(\omega_c)|\exp[i(\phi_\omega(\omega_c-\Omega) - \phi_\omega(\omega_c))] \tag{13}$$

and

$$D^{(+\mathrm{ac})}(\omega_c) = |\tilde{E}(\omega_c-\Omega)\tilde{E}(\omega_c)|\exp[-i(\phi_\omega(\omega_c-\Omega) - \phi_\omega(\omega_c))]. \tag{14}$$

The dc portion of the interferogram [see (12)] is the sum of the individual spectra of the pulses and contains no phase information. The ac terms [see (13) and (14)] are the result of the interference and contain all of the phase information.

There are three steps for reconstructing the spectral phase from the interferogram. First, isolate one of the ac terms, and hence $\phi_\omega(\omega_c-\Omega)-\phi_\omega(\omega_c)-\tau\omega_c$, with a Fourier transform and filter technique. Second, remove $\tau\omega_c$ by subtracting a calibration phase. Third, reconstruct $\phi_\omega(\omega_c)$ by concatenating the spectral phase difference.

To isolate the spectral phase difference, we use a robust algorithm introduced by Takeda *et al.* [13] in which the data is Fourier transformed with respect to the spectrometer frequency, filtered, and inverse transformed. The Fourier transform is

$$\tilde{D}(t) = FT\{D^{(\mathrm{dc})}(\omega_c);\omega_c\to t\} + FT\{D^{(-\mathrm{ac})}(\omega_c);\omega_c\to t+\tau\} + FT\{D^{(+\mathrm{ac})}(\omega_c);\omega_c\to t-\tau\}. \tag{15}$$

This time series has components centered near $t=\pm\tau$ as well as a component at $t=0$, as illustrated in Fig. 3. The component at $t=0$ is the Fourier transform of the dc portion of the interferogram. The $t=\pm\tau$ components arise from the Fourier transforms of the ac portions of the interferogram. If τ is sufficiently large, the $t=0$ and $\pm\tau$ components are well separated in time and, as a result, the unwanted dc and negative ac components can be removed by filtering. For this purpose, we use a fourth-order super Gaussian $H(t)$ of full width τ centered at $t=\tau$. The filtered signal

$$\tilde{D}^{\mathrm{filter}}(t) = H(t-\tau)\tilde{D}(t) = FT\{D^{(+\mathrm{ac})}(\omega_c);\omega_c\to t-\tau\} \tag{16}$$

is simply the Fourier transform of the positive ac portion $(t=+\tau)$ of the interferogram. The spectral phase difference is the argument of the inverse transform of $\tilde{D}^{\mathrm{filter}}(t)$

$$\phi_\omega(\omega_c)-\phi_\omega(\omega_c-\Omega)+\tau\omega_c = \arg\big[D^{(+\mathrm{ac})}(\omega_c)\big] = \arg[IFT\{\tilde{D}^{\mathrm{filter}}(t);t\to\omega_c\}]. \tag{17}$$

The second step of the phase reconstruction procedure is to remove the linear phase term $\tau\omega_c$ from (17). The most reliable method of doing this is with a direct measurement of $\tau\omega_c$. The interferometer is calibrated by recording a spectral interferogram for the pair of pulses without imparting the spectral shear. In this case, the interfered pulses are identical and therefore the only phase contribution is $\tau\omega_c$. The linear phase obtained from calibration is simply subtracted from $\phi_\omega(\omega_c) - \phi_\omega(\omega_c - \Omega) + \tau\omega_c$.

The third step is to reconstruct the spectral phase from the spectral phase difference. To simplify notation, we define the phase difference as $\theta(\omega_c)$

$$\theta(\omega_c) \equiv \phi_\omega(\omega_c) - \phi_\omega(\omega_c - \Omega). \tag{18}$$

$\phi_\omega(\omega_c)$ is reconstructed from $\theta(\omega_c)$ by concatenating the spectral phase difference. In practice, there is usually an unknown constant phase θ_0 associated with $\theta(\omega_c)$ which gives a linear contribution to the reconstructed spectral phase and results in an unimportant time-shift of the pulse. Although the time-shift is unimportant, we usually shift the entire phase difference data set by $-\theta(\omega_0)$ before reconstructing $\phi_\omega(\omega_c)$ so that the linear contribution is minimal.

Concatenation returns a sampled spectral phase at intervals of Ω across the spectrum. The spectral phase at some frequency, say ω_0, is set equal to zero so that $\phi_\omega(\omega_0 - \Omega) = -\theta(\omega_0)$. The spectral phase for all frequencies that are multiples of the spectral shear away from ω_0 follow in this fashion:

$$\begin{aligned}
&\vdots \\
\phi_\omega(\omega_0 - 2\Omega) &= -\theta(\omega_0 - \Omega) - \theta(\omega_0) \\
\phi_\omega(\omega_0 - \Omega) &= -\theta(\omega_0) \\
\phi_\omega(\omega_0) &= 0 \\
\phi_\omega(\omega_0 + \Omega) &= \theta(\omega_0 + \Omega) \\
\phi_\omega(\omega_0 + 2\Omega) &= \theta(\omega_0 + 2\Omega) + \theta(\omega_0 + \Omega) \\
&\vdots
\end{aligned} \tag{19}$$

By simply adding up the phase differences, we reconstruct the phase for frequencies separated by the spectral shear. By virtue of the Sampling Theorem discussed in Section I, this is sufficient information for reconstructing the electric field exactly.

If the shear is small relative to the structure of the spectral phase, the phase difference is approximately the first derivative of the spectral phase

$$\theta(\omega_c) \equiv \phi_\omega(\omega_c) - \phi_\omega(\omega_c - \Omega) \approx \Omega \frac{d\phi_\omega(\omega_c)}{d\omega_c}. \tag{20}$$

Accordingly, the spectral phase can be reconstructed by integration

$$\phi(\omega_c) \approx \frac{1}{\Omega} \int d\omega_c\, \theta(\omega_c). \tag{21}$$

There is little advantage to the integration approximation since the sampled phase returned from concatenation is adequate for reconstructing the electric field. It provides, however, a simple means of averaging over the many data sets available in a single interferogram. The spectral step size of the data is usually much smaller than the shear, and, consequently, concatenation uses only a subset of the available data. Integration, in contrast, uses all of the data. Of course, one can construct many sets of the sampled spectral phase by starting the concatenation at different frequencies, e.g., ω_0, $\omega_0 + \delta\omega_c$, $\omega_0 + 2\delta\omega_c \ldots$, then using each sampled set to reconstruct the analytic signal, and finally averaging the reconstructed analytic signals in the time domain.

The final step to reconstructing the electric field is to determine the spectral amplitude. The simplest way to do this is from a separate measurement of $|\tilde{E}(\omega_c)|$. Note that some applications, such as adaptive phase compensation, need only $\phi_\omega(\omega)$ and therefore do not require a separate measurement of the pulse spectrum.

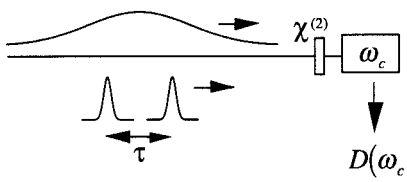

Fig. 4. The SPIDER apparatus. Two pulse replicas that are delayed with respect to one another by τ are frequency mixed with a chirped pulse in a nonlinear crystal. Each pulse replica is frequency mixed with a different time slice, and hence spectral slice, of the stretched pulse, and, consequently, the upconverted pulses are spectrally sheared. The resulting interferogram is resolved with a spectrometer.

IV. The SPIDER Apparatus

A. Generating the Spectral Shear with Nonlinear Frequency Mixing

The SPIDER apparatus is shown in Fig. 4. A test pair of pulses that are both identical to the input pulse and are delayed in time with respect to one another by τ are upconverted with a stretched pulse in a nonlinear crystal. A spectrometer resolves the frequency-mixed signal. The stretched pulse is severely chirped and consequently each pulse in the test pair is upconverted with a different frequency in the stretched pulse. As a result, the upconverted pulses are spectrally sheared with respect to one another. That is, nonlinear frequency mixing simulates a linear temporal phase modulator.

To quantify the shear, consider the action of a pulse stretcher in the form of a dispersive delay line. An ideal stretcher is a time-stationary quadratic spectral phase filter with transfer function

$$\tilde{S}_q^P(\omega) = e^{+i\frac{1}{2}\phi''(\omega-\omega_o)^2}. \tag{22}$$

The analytic signal of the stretched pulse is

$$\begin{aligned}
E_{\text{stretch}}(t) &= E_{\text{in}}(t) \otimes S_q^P(t) \\
&\propto e^{-i\frac{t^2}{2\phi''}} \int dt' E_{\text{in}}(t') e^{-i\frac{t'^2}{2\phi''}} e^{i\frac{tt'}{\phi''}}.
\end{aligned} \tag{23}$$

For large enough ϕ'', $t'^2/2\phi'' \approx 0$ for all t' over which the input pulse is nonzero. In this case, the analytic signal of the

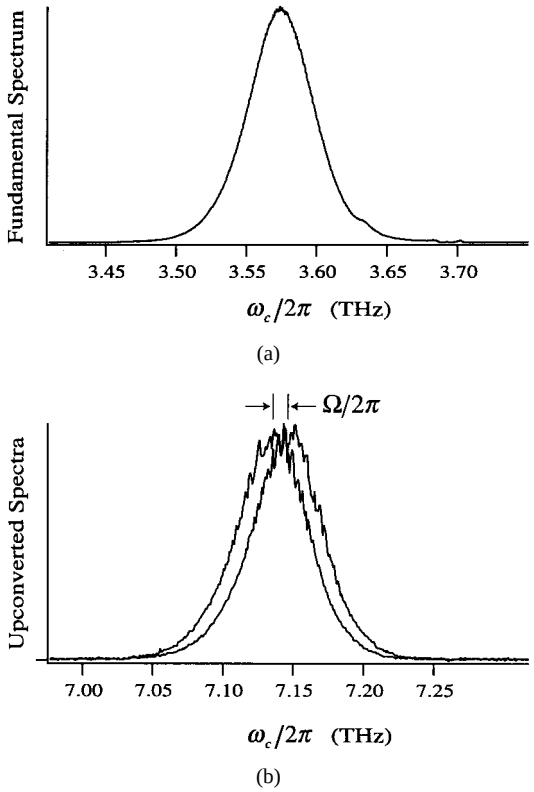

Fig. 5. (a) The fundamental and (b) upconverted spectra of pulses from our CW mode-locked Ti:sapphire oscillator. The upconverted pulses are frequency-shifted replicas of the input pulse. Since each is frequency mixed with a different quasi-monochromatic slice of a stretched pulse, the upconverted pulses are frequency sheared by Ω.

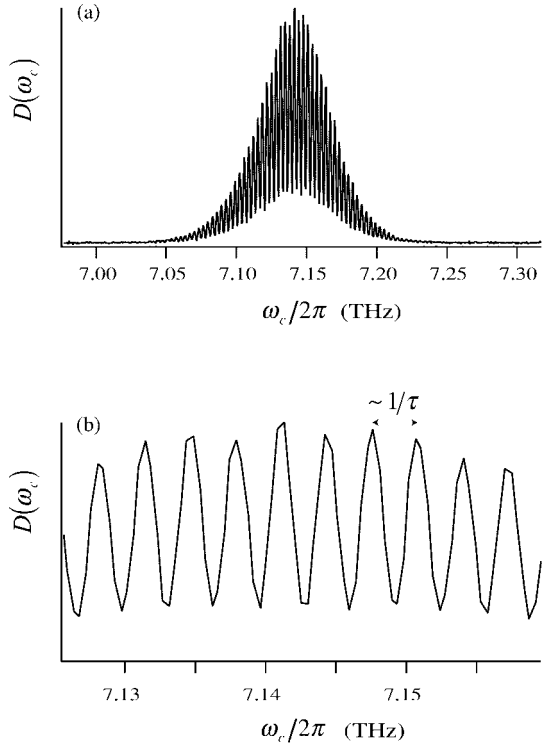

Fig. 6. (a) The experimental SPIDER interferogram recorded when the pulses of Fig. 5 are allowed to interfere. (b) The expanded view reveals that the fringes are nominally spaced at $1/\tau$ as expected.

stretched pulse is simply

$$E_{\text{stretch}}(t) \approx e^{-i\frac{t^2}{2\phi''}} \int dt' E_{\text{in}}(t') e^{i\frac{tt'}{\phi''}} = e^{-i(\omega_0 t + \frac{t^2}{2\phi''})} \tilde{E}_{\text{in}}\left(\omega = \omega_0 + \frac{t}{\phi''}\right). \quad (24)$$

For large quadratic dispersion, the pulse stretcher maps frequency into time.

As long as the large stretching approximation defined by (24) is satisfied, each pulse in the test pair is upconverted with a quasi-CW frequency slice of the stretched pulse. Thus, if the bandwidth of the nonlinear crystal is sufficiently broad, the analytic signals of the upconverted pulses are

$$E_1(t) \propto E_{\text{in}}(t) E_{\text{stretch}}(t) \approx E_{\text{in}}(t) e^{-i[\omega' + \Omega]t} \quad (25)$$

and

$$E_2(t) \propto E_{\text{in}}(t-\tau) E_{\text{stretch}} \approx E_{\text{in}}(t-\tau) e{-}i\omega'(t-\tau) \quad (26)$$

where $\omega' = \omega_0 - \Omega$ and $\Omega = -\tau/\phi''$. Note that ϕ'' is the value of the quadratic dispersion at the frequency with which the leading pulse is upconverted, in this case ω_0 ($\phi'' < 0$ for the stretcher arrangement described in the following section). Indeed, upconversion generates the spectral shear by simulating the linear temporal phase modulator of (7).

The spectra of the sheared pulses are centered near twice the carrier frequency of the input pulse, i.e., $2\omega_0$. Fig. 5 shows the spectra of the input pulse and the upconverted pulses from a SPIDER device for a CW mode-locked Ti:sapphire oscillator.

When the sheared pulses are interfered, the frequency-resolved signal is related to the input pulse by

$$\begin{aligned} D(\omega_c) &= |\tilde{E}_1(\omega_c) + \tilde{E}_2(\omega_c)|^2 \\ &= |\tilde{E}_{\text{in}}((\omega_c - \omega') - \Omega)|^2 + |\tilde{E}_{\text{in}}(\omega_c - \omega')|^2 \\ &\quad + 2|\tilde{E}_{\text{in}}((\omega_c - \omega') - \Omega)\tilde{E}_{\text{in}}(\omega_c - \omega')| \\ &\quad \times \cos[\phi_\omega((\omega_c - \omega') - \Omega) - \phi_\omega(\omega_c - \omega') - \tau\omega_c]. \end{aligned} \quad (27)$$

The experimental interferogram for the pulses of Fig. 5 is shown in Fig. 6. This interferogram is a frequency-shifted version of (10) and consequently the spectral phase is retrieved following the procedure of Section III-B.

B. Designing the SPIDER Apparatus

The two key parameters to be determined when designing a SPIDER apparatus are the spectral shear Ω and the relative delay between the pulses in the test pair τ. These are not independent since $\Omega = -\tau/\phi''$. Moreover, there are individual constraints on both parameters. For instance, since the fringes of the spectral interferogram are nominally spaced at $2\pi/\tau$, τ should not be so large that the fringes are not resolvable with the available spectrometer. But, τ should not be so small that the data inversion routine cannot separate the ac terms from the dc term. Likewise, Ω should not be so large that the phase sampling interval is larger than the Nyquist limit but it should not be so small that the spectral phase difference is imperceptible. The stretcher dispersion ϕ'' is also constrained. It must be sufficiently large to ensure that each pulse in the

test pair is upconverted with a quasi-CW slice of the stretched pulse. Of course, the required dispersion depends upon the spectral width $\Delta\omega$ and duration Δt of the input pulse.

For example, consider an input pulse typical of an ultrafast Ti:sapphire laser system, with spectral width $\Delta\omega = 2\pi \times 10$ THz centered at $\omega_0 = 2\pi \times 375$ THz ($\Delta\lambda \approx 21$ nm, $\lambda_0 = 800$ nm). Near transform limit, this pulse has a duration of $\Delta t \approx 50$ fs. For large stretching, the duration of the stretched pulse is $T \approx \Delta\omega\phi''$. If the duration of the input pulse is Δt, then a stretched pulse of duration $100 \times \Delta t$ ensures that each time slice of the stretched pulse has a range of frequencies no larger than $\Delta\omega/100$. In this example, since the input pulse might be longer than transform limit, the stretched pulse should be, say, 20 ps long ($T = 400 \times \Delta t$). The spectrometer must have adequate resolution to resolve the fringes at $2\pi/\tau$. If the spectrometer resolution is, say, $\gamma = \Delta\omega/100 = 2\pi \times 0.1$ THz (0.5 Å at $\lambda = 400$ nm), the delay τ must be less than 5 ps so that the spectrometer can resolve more than two points per fringe. The effects of uncorrelated noise diminish as the square root of the number of points per fringe, so one should choose optimally a delay less than 5 ps. On the other hand, the delay cannot be arbitrarily small because the inversion relies on the pulses being sufficiently separated in time to distinguish the ac and dc terms of the interferogram. Since the ac and dc terms have roughly the same duration as the input pulse, we usually choose the delay to be at least ten times the transform limit. Erring on the safe side, a delay of one to two picoseconds, $\tau \approx 1$ to 2 ps, resulting in five to ten points per fringe, is adequate in this example. This gives a spectral shear $\Omega = \Delta\omega\tau/T$ of 5%–10% of the input pulse spectral width, which satisfies the sampling criterion.

To generate the stretched pulse, we arrange a pair of diffraction gratings as a conventional compressor [14]. A prism pair or even simply a block of highly dispersive glass are suitable for ultrashort pulses with bandwidths of $\Delta\omega > 2\pi \times 25$ THz but are not practical for most applications. The gratings in our device are ruled with 1200 lines/mm. For the example pulse given above, these gratings allow for a compact geometry. A tandem pair of 1200 lines/mm gratings separated by approximately 10 cm will stretch the example pulse to 20 ps.

To generate the test pair of pulses, we use either the two reflections from an uncoated solid etalon or a Michelson interferometer. Interferometric accuracy unavoidably requires interferometric stability in τ since jitter between the test pulses can destroy all phase information. The source of most jitter is mechanical vibrations of frequencies of a few hundred hertz and less. A solid etalon is immune to these vibrations while a Michelson requires at least passive stabilization. The beamsplitter and both mirrors of our Michelson are mounted directly to a solid block of aluminum and the interferometer is enclosed in a plexiglass box. This passive stabilization is more than adequate for the laboratory environment. Of course, if the apparatus is operated single-shot, vibrations are not important. Note that the stretched pulse does not interfere with the test pair and therefore these relative paths do not need to be stabilized.

Both types of interferometers can be configured for low dispersion. For instance, a 150-μm fused silica solid etalon provides a 1.5-ps delay with minimal dispersion. Similarly, a thin beamsplitter imparts little dispersion in a Michelson (a pellicle can be used for extremely broad-band pulses). In either case, the spectral phase imparted by the substrate material is easily measured using conventional spectral interferometry [15], [16] for which the SPIDER apparatus is easily adapted.

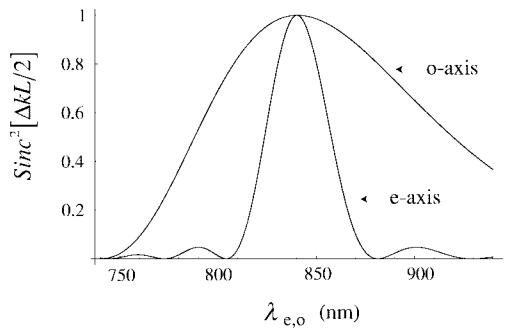

Fig. 7. Cross sections of the phase mismatch function for a 250-μm Type II BBO crystal. The crystal is cut for phase matching of $\lambda_o = 840$ nm and $\lambda_e = 840$ nm ($\theta = 40.25^0$). The bandwidth of the ordinary axis is considerably broader than that of the extraordinary axis. Consequently, the test pair of pulses should be polarized along the ordinary axis.

The test pair of pulses is frequency mixed with the stretched pulse in a nonlinear crystal. The bandwidth of the nonlinear crystal must be sufficiently large to upconvert all of the frequencies of the input pulse without imparting additional spectral phase. Moreover, the upconverted signal should not contain terms arising from the upconversion of the short pulses with themselves or from the stretched pulse with itself. Our apparatus uses a 250-μm type II BBO crystal. The type II crystal simplifies the geometry since the signal is background-free even if the test pair is collinear with the stretched pulse. Calculated cross sections of the phase-matching function along the ordinary and extraordinary axes of our crystal are shown in Fig. 7. The bandwidth along the ordinary axis is substantially larger than that along the extraordinary axes. Consequently, the test pair of pulses should be polarized along the former and the stretched pulse should be polarized along the latter. We use a zeroth-order half-wave plate to rotate the polarization of either the stretched pulse or the test pair, but a pair of mirrors will also suffice.

A photodiode at the output of a scanning monochromator or a CCD array at the output of a spectrometer is used to record the spectral interferogram. Our monochromator has a resolution of 0.5 Å and our spectrometer has a resolution of approximately 1 Å. Either instrument resolves the fringes at $2\pi/\tau$ for a delay of two picoseconds.

We measured the interferogram of Fig. 6 using our scanning monochromator. The time-dependent intensity and phase of these pulses is shown in Fig. 8 along with a comparison of the reconstructed and measured autocorrelation. The agreement between the reconstructed and measured autocorrelation is excellent. As an independent test, we also characterized the pulses after they propagated through a known amount of dispersion. The results of this test are shown in Fig. 9. Again, the agreement between the measured and predicted pulses is

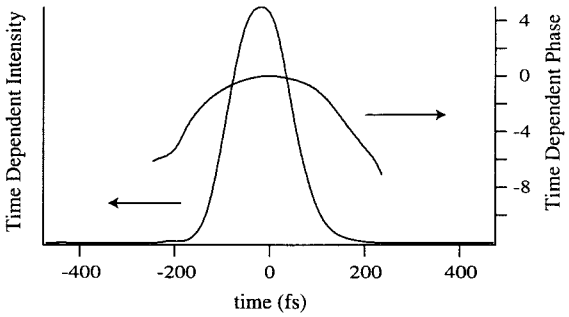

(a)

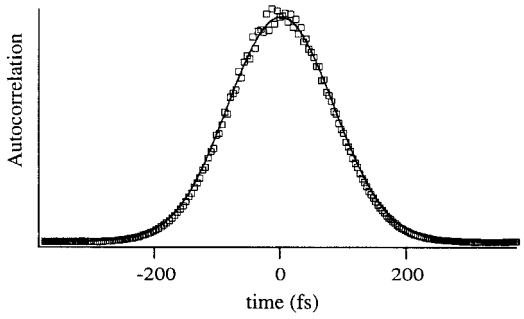

(b)

Fig. 8. (a) The time-dependent intensity and phase reconstructed from the SPIDER interferogram of Fig. 6. (b) The measured (boxes) and reconstructed (solid line) autocorrelation for the pulses of (a).

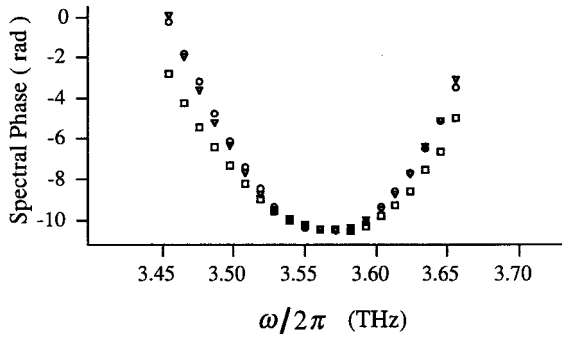

Fig. 9. The spectral phase returned by SPIDER for the pulses of Fig. 8 (squares) and for the same pulses after propagation through a dispersive piece of glass (triangles). The spectral phase predicted for the pulses upon propagation through the glass is also shown (circles).

excellent. Numerical simulations of SPIDER interferograms for more complicated pulses, such as those with phase discontinuities, show that the technique is easily capable of resolving pulse structure on the order of the spectrometer resolution.

C. Calibrating the Apparatus

The SPIDER apparatus must be calibrated. Since there are no moving components, this needs to be done only once at the initial setup. To take full advantage of the extreme sensitivity to phase offered by SPIDER, parts of the calibration need to be performed with interferometric accuracy. There are three steps to fully calibrate the device. First, the linear phase term $\omega\tau$ is determined from measurement of an interferogram without spectral shear. Second, the spectral shear Ω is determined either by direct measurement or simply by calculating the stretcher dispersion. Third, the frequencies of the quasi-CW slices of the stretched pulse with which each of the pulses in the test pair are upconverted are determined by comparing a SPIDER interferogram with the fundamental spectrum of the input pulse. This section addresses the details of each step of the calibration, provides estimates of the required accuracy, and points out self-consistency checks that allow the user to make certain that the apparatus is aligned and operating correctly.

The first and most important step of the calibration procedure is to determine the linear phase $\omega\tau$. The most reliable means of doing this is to directly measure the $\omega\tau$ contribution to the SPIDER interferogram. This is readily accomplished by recording the second-harmonic signal generated with the stretched pulse blocked and the polarization of the test pair of pulses rotated by 45° (or, equivalently, the Type II nonlinear crystal rotated by 45°). Since these two pulses are identical, that is, they are not spectrally sheared, the only phase contribution to the interferogram is the linear term $\omega\tau$ regardless of the phase of the input pulse. The second-harmonic calibration interferogram is analyzed in the same manner as the SPIDER interferogram up to concatenation. The resulting phase is the desired $\omega\tau$ term and is saved as a calibration trace so that it can later be subtracted from SPIDER data. Directly measuring the linear phase contribution is extremely accurate since the calibration uses the test pair of pulses which propagate through the entire SPIDER apparatus, and the same spectrometer and inversion procedure used for SPIDER data. Furthermore, this calibration procedure reduces the effects of dispersion in the device. For instance, it usually happens that the two pulses in the test pair are not identical. This is because one of the pulses passes through the substrate of the beamsplitter in the Michelson or the substrate of the etalon while the other does not. Approximately half of this effect is removed in the calibration since the spectral phase difference between the second-harmonic pulses is roughly half of the spectral phase difference between the fundamental pulses. Consequently, the calibration procedure eliminates half of the dispersive effects of the etalon or Michelson beamsplitter, making SPIDER a naturally low-dispersion device.

The second step of the calibration is to determine the spectral shear Ω. If a Michelson interferometer is used, the spectral shear is easily measured by blocking each of the test pulses one at a time and recording the individual upconverted spectra as in Fig. 5. If an etalon is used, the procedure is more involved. Since the spectral shear is a function of the separation of the test pair of pulses and the dispersion of the stretcher, i.e., $\Omega = -\tau/\phi''$, it is necessary to determine τ and ϕ''. τ is determined by measuring the slope of the linear spectral phase returned from the first step of the calibration. The simplest, and arguably most accurate, method for determining ϕ'' is by calculation. For instance, for a conventional tandem pair of gratings, the dispersion is determined by the separation of the gratings and the angle of incidence of the input beam [14], both of which can be precisely measured. The dispersion is sensitive to wavelength and therefore it is important to calculate ϕ'' for

a wavelength near the frequencies of the stretched pulse with which the test pair are to be upconverted. Because the stretcher typically stretches the pulse by a factor of several hundred, the spectral phase of the input pulse and the material dispersion of beamsplitters, lenses, etc., are negligible.

The accuracy with which the shear should be determined can be estimated by accounting for spectral shear error $\delta\Omega$ in the approximate expression for the spectral phase given in (21)

$$\phi_r(\omega) \approx \frac{1}{\Omega+\delta\Omega}\int d\omega\,\theta(\omega) \approx \phi_a(\omega) - \frac{\delta\Omega}{\Omega}\phi_a(\omega). \quad (28)$$

The fractional error in the reconstructed phase caused by error in the calibration of the spectral shear is simply equal to the fractional error of the shear. For instance, a 1% calibration error results in a 1% error of the reconstructed spectral phase. Since the spectral shear is determined from the separation of the test pair of pulses and the dispersion of the stretcher, the error in determining each of these two parameters should be minimized. τ can be determined from the slope of the linear spectral phase returned from the first step of the calibration with error of less than 1%. ϕ'' can be calculated with similar accuracy.

The third and final step of the calibration procedure is to determine the quasi-CW frequencies of the stretched pulse with which the test pair are upconverted. If a Michelson interferometer generates the test pair, the quasi-CW frequency with which each pulse is upconverted is readily determined by blocking one arm of the interferometer and recorded the resulting upconverted spectrum. ω' is determined by simply comparing the upconverted spectrum with the fundamental spectrum. In practice, we make the comparison by numerically cross-correlating the two data sets. This also provides a straightforward consistency check that the apparatus is set up properly. The upconverted and fundamental spectra should be identical with the exception that they are shifted in frequency with respect to one another. If the spectra are not identical, then the apparatus requires adjustment.

If an etalon is used to generate the test pair, ω' can be determined from the SPIDER data and the fundamental spectrum of the input pulse. The magnitude of the positive ac portion of the interferogram is proportional to $|\tilde{E}(\omega_c-\omega')\,\tilde{E}(\omega_c-\omega'-\Omega)|$ [see (13)]. To determine ω', the product $|\tilde{E}(\omega)\tilde{E}(\omega-\Omega)|$, constructed from the fundamental spectrum and knowledge of Ω, is compared to $|\tilde{E}(\omega_c-\omega')\tilde{E}(\omega_c-\omega'-\Omega)|$. Once again, this comparison also provides a straightforward consistency check of the apparatus since the products should be frequency shifted with respect to one another but otherwise identical. Note that since Ω depends upon ω' it may be necessary to iterate between the second and third steps of the calibration procedure in order to obtain the most precise values of these two quantities. But this procedure needs to be done only once at the initial setup of the apparatus.

Moreover, error in determining ω' results in little error in the reconstructed spectral phase. In fact, to first order, it introduces no error at all in the reconstructed spectral phase. To see this, consider a pulse whose actual spectral phase is $\phi_a(\omega) = \phi_a''(\omega-\omega')^2/2$. If the error in ω' is $\delta\omega'$, the reconstructed spectral phase is

$$\begin{aligned}\phi_r(\omega) &= \frac{1}{2}\phi_a''(\omega-\omega'-\delta\omega')^2 \\ &= \phi_a(\omega) - \phi_a''\delta\omega'(\omega-\omega') + \frac{1}{2}\phi_a''\delta\omega'^2. \end{aligned} \quad (29)$$

The error that is linear with frequency is an error in the determination of the time of arrival of the input pulse, while the constant error is in the determination of the absolute phase of the input pulse. SPIDER does not return either of these quantities and, consequently, the errors are meaningless. The error in ω' is meaningful if the actual spectral phase has terms of order greater than quadratic. But, a similar argument to that of (29) reveals that the tolerance on ω' is not stringent—if the spectral phase is dominated by cubic phase, an error in ω' of 5% of the test pulse bandwidth results in an error of the reconstructed spectral phase of less than 1%.

V. Summary

Spectral phase interferometry for direct electric-field reconstruction (SPIDER) is a simple and reliable interferometric technique for measuring the electric field underlying an ultrashort optical pulse. The data inversion algorithm is direct (noniterative), and the amount of data is much less than that required by spectrographic and tomographic techniques. The SPIDER apparatus has no moving components. Moreover, since SPIDER uses a Type II nonlinear crystal, the apparatus is entirely collinear and background-free. Also, there is no ambiguity as to the direction of time of the reconstructed pulse even using a lowest order nonlinearity.

We presented in this paper experimental examples of reconstructed pulses from a CW mode-locked Ti:sapphire oscillator [17]. We have also used a similar SPIDER device to measure pulses from an amplified Ti:sapphire system, and, by using nonlinear downconversion instead of upconversion, we have characterized the pulses at the second harmonic of this system [18]. SPIDER has also been used in the feedback loop for adaptive phase control of amplified pulses [19]. We are currently developing both a device with real-time updating to take advantage of the rapid data inversion algorithm of SPIDER, and, since SPIDER requires only 1-D data collection for pulse reconstruction at a single spatial coordinate, a device with a 2-D CCD camera for measuring the electric field as a function of both space and time.

References

[1] I. A. Walmsley and V. Wong, "Characterization of the electric field of ultrashort optical pulses," *J. Opt. Soc. Amer. B*, vol. 13, pp. 2453–2463, 1996.

[2] C. Iaconis, V. Wong, and I. A. Walmsley, "Direct interferometric techniques for characterizing ultrashort optical pulses," *IEEE J. Select. Topics Quantum Electron.*, vol. 4, pp. 285–294, 1998.

[3] D. J. Kane and R. Trebino, "Characterization of arbitrary femtosecond pulses using frequency-resolved optical gating," *IEEE J. Quantum Electron.*, vol. 29, pp. 571–579, 1993.

[4] V. Wong and I. A. Walmsley, "Ultrashort-pulse characterization from dynamic spectrograms by iterative phase retrieval," *J. Opt. Soc. Amer. B*, vol. 14, pp. 944–949, 1997.

[5] J. L. A. Chilla and O. E. Martinez, "Direct determination of the amplitude and the phase of femtosecond light pulses," *Opt. Lett.*, vol. 16, pp. 39–41, 1991.

[6] J.-K. Rhee, T. S. Sosnowski, A.-C. Tien, and T. B. Norris, "Real-time dispersion analyzer of femtosecond laser pulses with use of a spectrally and temporally resolved upconversion technique," *J. Opt. Soc. Amer. B*, vol. 13, pp. 1780–1785, 1996.
[7] H. R. Lange, M. A. France, J. F. Ropoche, B. S. Prade, P. Rousseau, and A. Mysyrowicz, "Reconstruction of the time profile of femtosecond laser pulses through cross-phase modulation," *J. Select. Topics Quantum Electron.*, vol. 4, pp. 295–300, 1998.
[8] S. Prein, S. Diddams, and J.-C. Diels, "Complete characterization of femtosecond pulses using an all-electronic detector," *Opt. Commun.*, vol. 123, pp. 567–573, 1996.
[9] K. C. Chu, J. P. Heritage, R. S. Grant, K. X. Liu, A. Dienes, W. E. White, and A. Sullivan, "Direct measurement of the spectral phase of femtosecond pulses," *Opt. Lett.*, vol. 20, pp. 904–906, 1995.
[10] V. A. Zubov and T. I. Kuznetsova, "Solution of the phase problem for time-dependent optical signals by an interference system," *Sov. J. Quantum Electron.*, vol. 21, pp. 1285–1286, 1991.
[11] V. Wong and I. A. Walmsley, "Analysis of ultrashort pulse-shape measurement using linear interferometers," *Opt. Lett.*, vol. 19, pp. 287–289, 1994.
[12] J. W. Goodman, *Introduction to Fourier Optics*. New York: McGraw-Hill, 1988, ch. 2.
[13] M. Takeda, H. Ina, and S. Kobayashi, "Fourier-transform method of fringe-pattern analysis for computer-based topography and interferometry," *J. Opt. Soc. Amer.*, vol. 72, p. 156, 1982.
[14] E. B. Treacy, "Optical pulse compression with diffraction gratings," *IEEE J. Quantum Electron.*, vol. QE-5, pp. 454–458, 1969.
[15] C. Froehly, A. Lacourt, and J. C. Vienot, "Time impulse response and time frequency response of optical pupils. Experimental confirmations and applications," *J. Opt.*, vol. 4, p. 183, 1973.
[16] F. Reynaud, F. Salin, and A. Barthelemy, "Measurement of phase shifts introduced by nonlinear optical phenomena on subpicosecond pulses," *Opt. Lett.*, vol. 14, p. 275, 1989.
[17] C. Iaconis and I. A. Walmsley, "Spectral phase interferometry for direct electric-field reconstruction of ultrashort optical pulses," *Opt. Lett.*, vol. 23, pp. 792–794, 1998.
[18] ———, "Characterizing ultrashort optical pulses from the uv to the ir using SPIDER," in *OSA Annu. Conf.*, Baltimore, MD, 1998.
[19] C. Dorrer, F. Salin, C. Iaconis, and I. A. Walmsley, "Characterization of femtosecond kHz amplifier chains by spectral shearing interferometry," in *Conf. Lasers and Electro-Optics*, San Francisco, CA, 1998.

Chris Iaconis received the B.Sc. degree in engineering physics from the University of Colorado, Boulder. He is currently working toward the Ph.D. degree at the Institute of Optics, University of Rochester, Rochester, NY.

Ian A. Walmsley was born in the U.K. He received the B.Sc. degree in physics from Imperial College, University of London, U.K., and the Ph.D. degree in optics from the Institute of Optics, University of Rochester, Rochester, NY.

After a post-doctoral position at Cornell University, Ithaca, NY, he joined the faculty of the Institute of Optics, where he is currently a Professor. His research interests are in ultrafast optics, especially as applied to fundamental problems in quantum control and state measurements and in quantum optics.

He is a fellow of the Optical Society of America.